THE JOURNAL OF PHYSICAL CHEMISTRY A

Article

pubs.acs.org/JPCA

Structural Exploration of Water, Nitrate/Water, and Oxalate/Water Clusters with Basin-Hopping Method Using a Compressed Sampling Technique

Yi-Rong Liu,[†] Hui Wen,[†] Teng Huang,[†] Xiao-Xiao Lin,[†] Yan-Bo Gai,[†] Chang-Jin Hu,[†] Wei-Jun Zhang,*[,†,‡] and Wei Huang*[,†,‡]

[†]Laboratory of Atmospheric Physico-Chemistry, Anhui Institute of Optics & Fine Mechanics, Chinese Academy of Sciences, 350 Shushan Lake Road, Hefei, Anhui 230031, China

[‡]School of Environmental Science & Optoelectronic Technology, University of Science and Technology of China, 96 Jinzhai Road, Hefei, Anhui 230026, China

Supporting Information

ABSTRACT: Exploration of the low-lying structures of atomic or molecular clusters remains a fundamental problem in nanocluster science. Basin hopping is typically employed in conjunction with random motion, which is a perturbation of a local minimum structure. We have combined two different sampling technologies, "random sampling" and "compressed sampling", to explore the potential energy surface of molecular clusters. We used the method to study water, nitrate/water, and oxalate/water cluster systems at the MP2/aug-cc-pVDZ level of theory. An isomer of the $NO_3^-(H_2O)_3$ cluster molecule with a 3D structure was lower in energy than the planar structure, which had previously been reported by experimental study as the lowest-energy structure. The lowest-energy structures of the $NO_3^-(H_2O)_5$ and $NO_3^-(H_2O)_7$ clusters were found to have structures similar to pure $(H_2O)_8$ and $(H_2O)_{10}$ clusters, which contradicts previous experimental result by Wang et al.(*J. Chem. Phys.* **2002**, *116*, 561−570). The new minimum energy structures for $C_2O_4^{2-}(H_2O)_5$ and $C_2O_4^{2-}(H_2O)_6$ are found by our calculations .

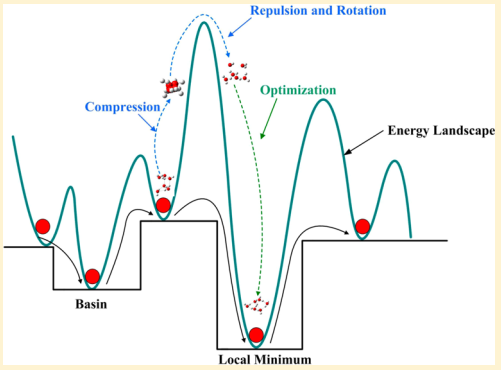

I. INTRODUCTION

Nanoclusters are small groups of atoms or molecules whose sizes range between those of individual atoms and condensed matter. The cluster properties strongly depend on their structures. Examining the low-lying structures of a complex potential energy surface (PES) remains a fundamental problem in the field of cluster science. For example, to scrutinize the properties of a nanoparticle or to find the low-lying structures of a gold colloid, one must find the global minima on a PES. Various techniques have been used to explore nanocluster structures, such as photoelectron spectroscopy,[1] ion mobility,[2,3] infrared multiphoton dissociation spectroscopy,[4,5] and trapped ion electron diffraction.[6] These techniques are quite powerful in obtaining structural information when combined with ab initio calculations.

For atomic or molecular clusters, the number of local minima and the calculation costs increase rapidly with the cluster size.[7,8] Determining the minimum-energy structure on a multidimensional PES is difficult if the cluster has a large number of minima separated by high-energy barriers. Finding the global minimum on a complicated PES via a manual search is impossible. The potential energy landscapes of many interesting cluster systems are complicated with enormous numbers of minima containing the degenerate states of various structures. To find the global minimum, we must screen the high-dimensional PES using different strategies, one of which creates an effective searching algorithm to accurately describe the characteristics of the PES. The algorithm aims to rapidly obtain a large number of different low-energy structures for a cluster molecule on a PES. Effectively describing the PES characteristics and rapidly generating a reasonable geometry for further optimization remains a challenging problem for structure-searching algorithms. In the last few decades, several algorithms have been developed for global optimization, such as genetic algorithms (GAs),[9−16] simulated annealing (SA),[17] basin hopping (BH),[18] and so on. These powerful algorithms can determine the structures of atomic or molecular clusters, but identifying the energetically similar isomers and searching large systems of atomic or molecular clusters remains difficult.[19] The BH algorithm essentially combines the Metropolis sampling technique and local optimization procedures using the same principle as the Monte Carlo minimization algorithm of Li and Scheraga.[20] This method has proven to be an effective stochastic global search algorithm. Recently, variants of the BH

Received: November 6, 2013
Revised: December 29, 2013
Published: December 30, 2013

method have been proposed[21−28] to further strengthen the technique. Molecular clusters could prove important in many fields, such as the atmospheric nucleation primarily related to molecular clusters[29−36] and gas-phase ion reactions.[37] An effective global minimum search algorithm is needed for molecular clusters.

The BH algorithm was used to determine the different molecular cluster systems, such as water, oxalate + water, and nitrate + water clusters, to demonstrate that this method can be used to determine the possible low-lying cluster structures of different sizes. The BH algorithm can be easily combined with many quantum chemistry packages such as DMol3 code,[38] the Gaussian 09 package,[39] the NWChem package,[40] and so on. We combined the BH method with density functional theory to explore the structure of $(H_2O)_n$ (n = 4−10), $C_2O_4^{2-}(H_2O)_n$ (n = 1−6), and $NO_3^-(H_2O)_n$ (n = 1−7) cluster systems, which are important in atmospheric nucleation.[41−53] Water is the most important solvent in the formation of atmospheric ice and clouds.[54] Previous studies have utilized different techniques to explore the structures and properties of water clusters.[55−86] Nitrate (NO_3^-) is a general inorganic anion in both the solid state and solution. Various techniques may be employed to discern the structure and solvation of NO_3^- (a gaseous anion common in the atmosphere[87]) in bulk solution, including neutron and X-ray diffractions.[88−90] The NO_3^- anion can react with water, which is present in relatively high concentration, to form molecular clusters in the atmosphere. Few theoretical calculations and experiment have been undertaken on the structure of $NO_3^-(H_2O)_n$ (n = 1−3).[91−97] The $C_2O_4^{2-}$ anion can exist in solutions and solids; however, isolated $C_2O_4^{2-}$ is unstable due the strong Coulombic repulsion between the two excess charges. Water can stabilize the oxalate dianion through a water−anion interaction. The hydrate oxalate dianion has been studied using experimental methods, and few theoretical calculations have examined the structure of $C_2O_4^{2-}(H_2O)_n$ (n = 1−6).[98−101] Oxalic acid is the most prevalent dicarboxylic acid in the atmosphere and effectively binds with sulfuric acid, the dominant nucleating species in the atmosphere.[102−105]

II. METHODS

The original BH algorithm essentially combines the Metropolis random sampling technique and local optimization procedures.[18] The BH method includes two steps: First, a new structure is generated via the random displacement of atoms; then, the structure is optimized to the local minimum. Second, this local energy minimum is used as a criterion to accept the initial generated structure spaces with Boltzmann weight at a finite temperature. This method essentially removes the effect of the transition-state regions without altering the global minimum. However, the efficiency of the BH algorithm depends heavily upon the effective sampling, causing the cluster to escape the local minimum and to shift to a new energy basin via finite steps. Effective sampling techniques are necessary for the BH algorithm. We have previously utilized the BH program with random sampling to study atomic clusters.[19,106−109]

In the original BH algorithm, a new coordinate is generated via random sampling (Figure 1A).[18] The maximum value of the random sampling at each atom or molecule remains constant. The atom or molecule on the surface of the cluster has a higher energy than the atom or molecule inside the cluster. So, the size of a randomly moving atom or molecule inside the cluster differs from that of an atom or molecule on the surface.

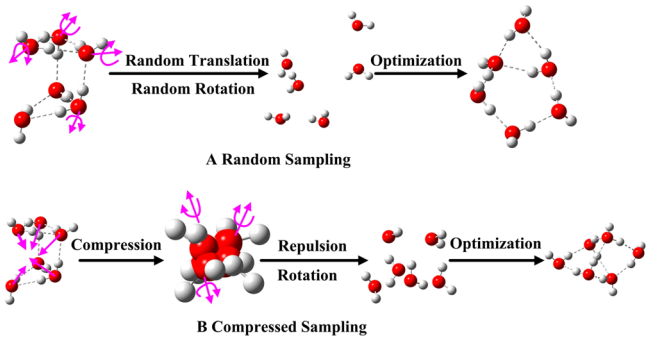

Figure 1. Two different sampling techniques for molecular clusters: random sampling (A) and compressed sampling (B).

Therefore, the atom or molecule with the higher relative energy in the cluster should exhibit greater movement and is more likely to move to a position of low energy within the cluster. The size of the atomic or molecular movement on the surface should be larger than that inside the cluster, which can lead to a reduction in the total energy of the cluster. To obtain a different sampling size, we use a new sampling technique called "compressed sampling" (Figure 1B) according to the following detailed procedures:

(1) Calculate the geometric center of the system.
(2) Calculate the distance D_i from the geometric center to an ith atom or molecule.
(3) Compress the atom or molecule relative to the geometric center of the system. The compression distance is proportional to D_i. (In general, the value of the compression distance is $0.7D_i$ in our program.)
(4) Allow each atom or molecule to repulse (translate) and rotate. The value of the translation on the surface is greater than that inside. The value of the rotation is 0 to $\pi/2$ for each molecule.
(5) Apply the conjugated gradient method to obtain a new configuration via "compressed sampling."
(6) Accept or refuse a new structure according to the Metropolis rule.

A continuous random perturbation is used to force the cluster to escape from one basin to another. When the typical compressed samples are rejected several times, the system is considered to be trapped at the local minimum. The temperature is raised to $T = \infty$, and the continuous random moves are executed several times to allow the system to escape the local minimum (Figure 2) according to the same principle as the escape strategy of Hainam Do.[110]

Initially, the molecules are generated randomly in a 3D coordinate space. To make a reasonable initial guess, the structure has been compressed and relaxed via repulsion and rotation. The repulsion and rotation will be executed when the distance between molecules drops below a threshold R, which is an empirical parameter. For a water cluster, R = 2 Å, but the value can change depending on the calculation system. For example, the water cluster combines through hydrogen bonding. According to our calculation at the BLYP/DNP level, the hydrogen bond length changes from 1.8 to 2.5 Å. Therefore, we choose 2 Å as the minimum threshold for a water cluster. The value can be altered by the user. The rotation is set from 0 to $\pi/2$. The choice of threshold value is important for the cluster structure search. If the value is too large or too small, the self-consistent filed (SCF) calculation will fail to

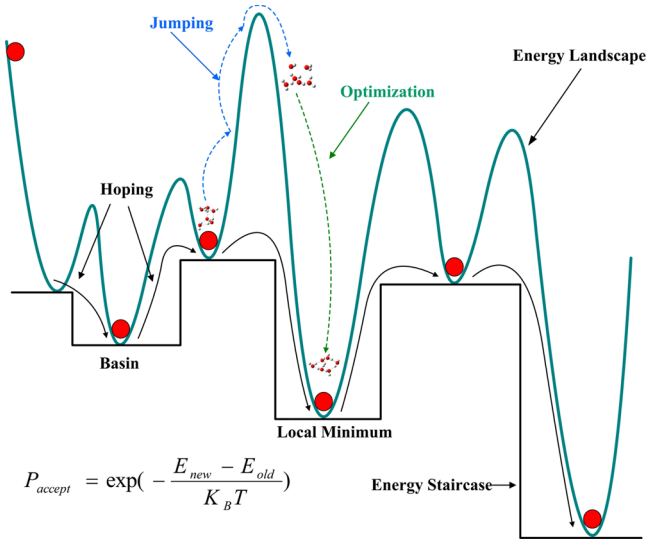

Figure 2. Schematic diagram of the basin-hopping algorithm for a 1D energy landscape.

converge requiring additional calculation time to optimize the structure. Previous studies have indicated that the translation and rotation of the molecule are important for a global search of molecular clusters.[111] We also use two different operations on each molecule via repulsion and rotation. When the system is trapped in the basin, a continuous random perturbation is executed. The program will automatically judge whether the sampling structure has a reasonable configuration for further optimization. If the distance between a molecule and its closest neighbor within a cluster exceeds 3 Å, the molecule will be considered separate. The program will then automatically draw the molecule closer to avoid the excessive distance that can result in the SCF calculation failing to converge, which requires additional time for structural optimization. For a water cluster, we believe that no interaction occurs between molecules when the distance exceeds 3 Å, which is also an empirical parameter and depends on the calculation system. We set two threshold parameters, 2 Å for the minimum distance and 3 Å for maximum distance at which the cluster molecule relaxes via repulsion and rotation. Finally, the distance between the molecules will be held between 2 and 3 Å for further structural optimization of the water molecule clusters. Therefore, controlling the distance between the molecules is critical for any sampling technique because molecules that are too close or too far will result in a failure of the optimization calculation and require additional computation time. The selection of reasonable intermolecular distances will save a great deal of computational time. The aforementioned method is effective for unconstrained sampling. To obtain a reasonable sampling structure for water clusters, we choose different threshold parameters with a minimum intermolecular distance of 1.8 to 2 Å and a maximum distance of 2.5 to 3 Å. The detail of how to set the search parameter of water, nitrate/water, and oxalate/water clusters in our program can be obtained in Table S1 in the Supporting Information (SI).

We performed a BH global minimum search combined with a DFT geometric optimization using DMol3 code[38] to obtain the low-lying structure of water, oxalate + water, and nitrate + water cluster systems. Because these systems are combined via hydrogen bonding, the BLYP exchange-correlation functional and the double-numerical polarized (DNP) basis set were employed for the geometric optimization in the DMol3 code.[38] Previous studies have indicated that the BLYP functional with the DNP basis set can reasonably describe the structural properties of hydrogen systems.[112] For each cluster, eight separate BH searches, consisting of 600 sampling steps at 1000 K starting with various randomly generated molecular configurations, were performed. For BH search, the structural optimization uses four central processing units (CPUs), and each CPU shares 2GB memory. The total calculation time of 600 BH steps with the cluster with different size can be found

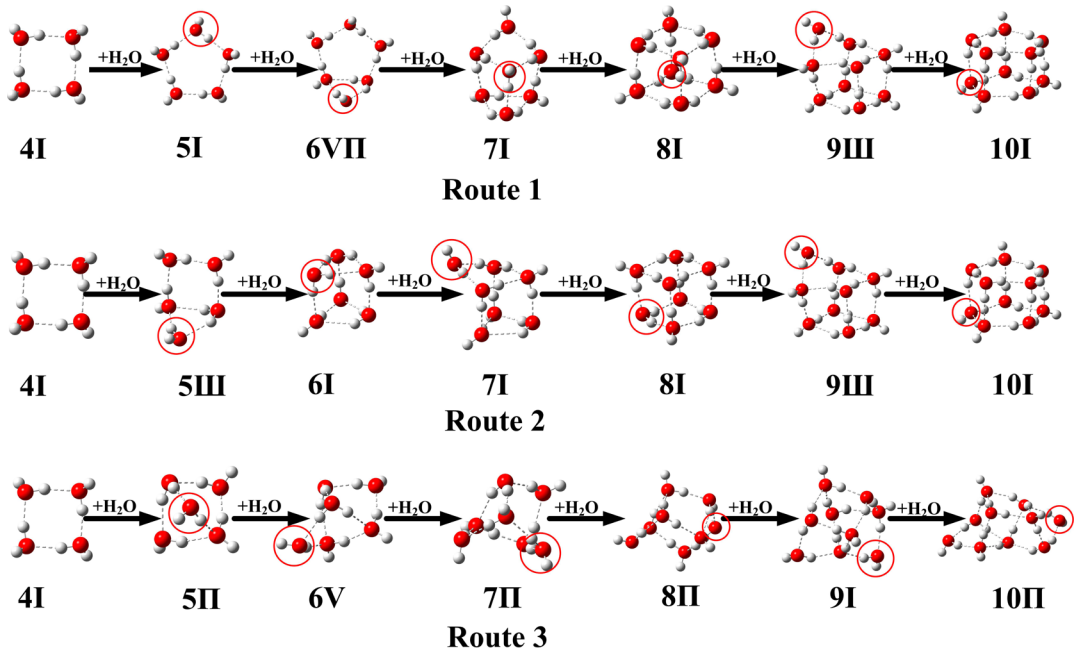

Figure 3. Structural evolution of the clusters from n = 4 to 10. Three difference structural evolutionary paths are depicted. The inset red rings indicate added water molecules.

in Figure S1 in the SI. In the BH algorithm, temperature plays a key role, driving the sampling of the configuration space according to the Boltzmann distribution. At each compressed sampling step, all molecules are repulsed and rotated. To obtain different isomer populations in the initial BH searches, we selected a medium-level convergence criterion such that the optimization gradient convergence was below 3×10^{-4} hartree/Å and the optimization energy convergence was 1×10^{-4} hartree in the DFT calculations. Different isomeric structures were collected, and the isomers were ranked according to their relative energies. The low-energy candidates obtained in the BH search were reoptimized at the MP2/aug-cc-pVDZ level, and the relative energies of the clusters were determined using B3LYP calculations with the aug-cc-pVTZ basis set via the NWChem software package.[40] To compare the results with the measured PES spectra of the $NO_3^-(H_2O)_3$ cluster, the first vertical detachment energy (VDE) of the $NO_3^-(H_2O)_3$ cluster was computed (at the B3LYP/aug-cc-pVTZ level of theory implemented in the NWChem software package[40]). The binding energies of the deeper orbitals were then added to the first VDE to yield VDEs for the excited states. Each VDE was fitted with a 35 meV wide Gaussian curve to simulate the density of states (DOS) spectra.

III. RESULTS AND DISCUSSION

A. Water Clusters. The lowest-energy structures for the $(H_2O)_n$ (n = 4−10) clusters predicted using MP2/aug-cc-pVDZ are depicted in Figure S2 in the SI, and three possible evolution routes are presented in Figure 3. All isomer structures can be found in the SI (Figures S3−S9).

For $(H_2O)_4$ and $(H_2O)_5$, the lowest-energy structures (4I in Figure S3 and 5I in Figure S4 in the SI) are cyclic rings, which is in agreement with previous studies.[76−81,83,110,113] The George group validated these two lowest-energy structures by comparing theoretical calculation with high-resolution IR spectroscopy.[80] For the $(H_2O)_5$ cluster, structures exhibiting hexahedral and vertical square-edge features are the two second-lowest-lying structures noted as 5II (Figure S4 in the SI) and 5III (Figure S4 in the SI), respectively, and connect two different evolution routes. According our experience, the global minimum structure of M_{N+1} usually can be found come from one of the low-lying isomers of M_N.[114−116] One can also speculate that the two low-lying structures marked 5II and 5III could exist under real experiment conditions. The two low-lying isomers can reasonably connect two different evolution routes with energies of 0.020 and 0.027 eV and are approximately the lowest cyclic ring structures. Many theoretical and experimental studies have been conducted using $(H_2O)_6$,[75−79,81,113,117−119] and different levels of theory and experimental conditions have led to different results regarding the lowest-energy structure. We have confirmed all reported structures for the $(H_2O)_6$ cluster from each search using our BH algorithm. These structures include trigonal prisms (6I in Figure S5 in the SI), book-like structures (6II in Figure S5 in the SI), cages (6 V in Figure S5 in the SI), and cyclic rings (6VI in Figure S5 in the SI). The trigonal prism is the lowest-energy structure at the MP2/aug-cc-pVDZ level, which is in agreement with the literature.[75,76,110]

For $(H_2O)_7$, an edge-capped trigonal prism (7I in Figure S6 in the SI) is the lowest-energy structure. This structure contains 10 hydrogen bonds, the largest number of hydrogen bonds that $(H_2O)_7$ can form, which also agrees with the previous study.[74,110,113] Other low-lying structures have been found such as the cage structure (7II in Figure S6 in the SI), a cube-like structure (7IV in Figure S6 in the SI), and a basket-like structure (7 V in Figure S6 in the SI). The cube-like structure (8I in Figure S7 in the SI) is the lowest-energy structure for $(H_2O)_8$ with D_{2d} symmetry and 12 hydrogen bonds, which is in good agreement with previous theoretical and experimental studies.[66,77−79,84,85,110,113] Other isomers, including the cage (8II in Figure S7 in the SI), butterfly-like (8IV in Figure S7 in the SI), and basket-like (8VII in Figure S7 in the SI) isomers, were also noted. For $(H_2O)_9$, a cage structure was found and assigned as the lowest-energy structure. Other low-lying structures (such as 9II (Figure S8 in the SI) and 9III (Figure S8 in the SI) presented in Figure S8 in the SI) were also found, which is consistent with other studies.[66,77,78,110,112,113] However, isomer 9II was assigned as the lowest-energy structure in previous work.[110] Other low-lying structures (Figure S8) can be found in the SI. For n = 10, a double-five-membered-ring stacked structure (10I in Figure S9 in the SI) was found to be the lowest-energy isomer with 15 hydrogen bonds. This result is in agreement with all previous theoretical studies.[66,110,112] The butterfly structure 10 V has also been found in previous experimental studies;[66] however, this structure appears to be 0.363 eV higher in energy than the lowest-energy structure in our work.

Three different evolutionary routes for the $(H_2O)_n$ (n = 4−10) clusters are proposed in Figure 3. The first route yields a 2D−3D structural transformation at n = 6, while the relative energy of the structure denoted 6VII (Figure S5 in the SI) is higher than the lowest-energy structure (6I in Figure S5 in the SI) within the $(H_2O)_6$ cluster molecule. As depicted in the first route, the main structures are those of lowest-energy within each cluster size from n = 4 to n = 10 except 6VII and 9III (Figure S8 in the SI). Thus, we can infer that the relatively high-energy structures of 6VII and 9III may also exist under real experimental conditions if the experimental parameters are reasonably controlled. Compared with the first route, the structural transformation from 2D−3D begins with n = 5 in the second route. We can clearly observe the evolutionary process from n = 4 to 10 by the increase in water molecules. The 5III (Figure S4 in the SI) and 9III (Figure S8 in the SI) isomers are higher in energy than the corresponding lowest-energy structures. For the third route, the cage-like structures appear to be the main evolutionary structures. A cage-like structure has also been experimentally proven to be favorable for $(H_2O)_6$.[118] These routes may coexist with different competition ratios. For each route, only a few structures have been observed experimentally. Each cluster size has different isomers from n = 4 to 10 in a different evolutionary process. In principle, the growth of the cluster structure can be viewed as a gradual process. The lowest-energy structure for each cluster size should have an embryo, which may result from an isomer of a smaller neighboring cluster, although this isomer may not have the lowest energy. The participation of the higher-energy isomer in the growth of the cluster may imply that different isomers with the same cluster size can exist with varying probabilities. In fact, a similar evolution trend was reported in our previous atomic-cluster studies.[115]

B. Nitrate + Water Clusters. The geometries of the $NO_3^-(H_2O)_n$ (n = 1−7) clusters have also been determined using the BH algorithm at the BLYP/DNP level. Because the cluster system is held together by hydrogen bonds, the low-energy structure candidates were reoptimized at the MP2/aug-cc-pVDZ level. The lowest-energy structure for each cluster is

provided in Figure 4. The first VDEs of the anion clusters were calculated at the B3LYP/aug-cc-pVTZ level (Table 1). The

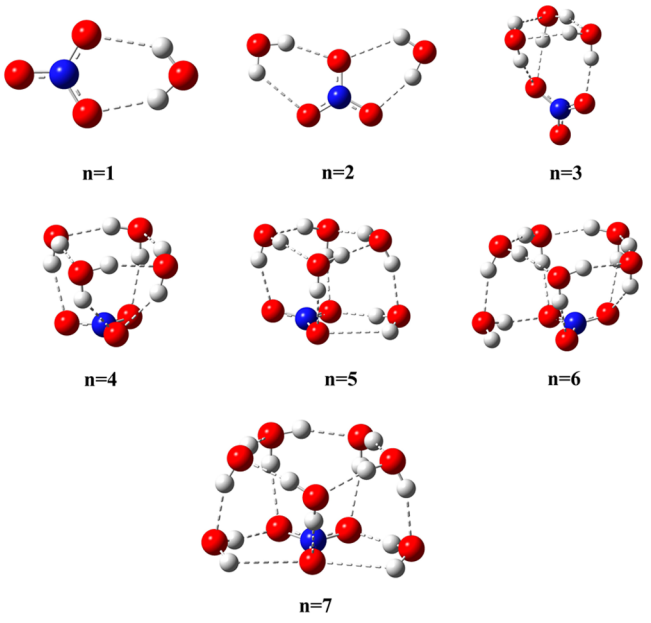

Figure 4. Lowest energy structures of the $NO_3^-(H_2O)_n$ (n = 1–7) clusters. The dashed lines represent hydrogen bonds.

Table 1. Experimental and Calculated Values [in electronvolts (eV)] of the First Vertical Detachment Energies (VDEs) of $NO_3^-(H_2O)_n$ Clusters (n = 1–7)[a]

		VDE	
cluster	N_{HB}	theor	expt[b]
$NO_3^-(H_2O)_1$	2	4.83	4.6(2)
$NO_3^-(H_2O)_2$	4	5.53	5.2(2)
$NO_3^-(H_2O)_3$	6	5.57	5.7(2)
$NO_3^-(H_2O)_4$	8	5.76	5.9(2)
$NO_3^-(H_2O)_5$	10	6.05	6.1(3)
$NO_3^-(H_2O)_6$	11	6.28	
$NO_3^-(H_2O)_7$	14	6.46	

[a]Numbers in parentheses represent the uncertainties in the last digit. All theoretical values were calculated at the B3LYP/aug-cc-pVTZ level. The N_{HB} values represent the number of hydrogen bonds for the $NO_3^-(H_2O)_n$ clusters (n = 1–7). The isomer information for each cluster size can be found in the SI. [b]Ref 120.

VDE is defined as the difference between the energies of the neutral and anion species. The theoretical VDEs of the lowest-energy structures for each cluster size are summarized in Table 1 along with other experimental parameters.[120] To further confirm the structural information for the $NO_3^-(H_2O)_3$ cluster, we simulated the photoelectron spectra of the $NO_3^-(H_2O)_3$ cluster at the B3LYP/aug-cc-pVTZ level (Figure 5). The 3D structure (3I in Figure S10 in the SI) was lower in energy than the planar structure with the lowest energy according to previous calculations.[95,120]

The $NO_3^-(H_2O)$ has only one possible structure (1I in Figure S10 in the SI) consisting of a water molecule hydrogen bonded to the nitrate oxygen to form two hydrogen bonds. This structure agrees with the previous theoretical studies found in the literature.[95−97,120−122] We can clearly observe a blue shift in the experimental spectrum with the added water molecule.[120] The hydrogen bond can shift the spectrum of the NO_3^- anion.

According to our calculations, $NO_3^-(H_2O)_2$ has two different isomers (2I and 2II in Figure S10 in the SI). All optimization was performed at the MP2/aug-cc-pVDZ level. The lowest-energy structure is flat (2I in Figure S10 in the SI) with the two hydrogen atoms from the water molecule forming two hydrogen bonds. The second isomer labeled 2II (Figure S10 in the SI) is 0.055 eV higher in energy than the lowest structure (2I in Figure S10 in the SI). The VDE of the lowest-energy structure (2I) is 5.53 eV, which is much higher than the experimental value of 5.2(2) eV. This structure agrees with the previous theoretical studies found in the literature.[95,96,120,122] For $NO_3^-(H_2O)_3$, the lowest-energy structure (3I in Figure S10 in the SI) is cage-like with a VDE of 5.57 eV and theoretical spectrum shape that is consistent with the experimental spectrum.[120] The other $NO_3^-(H_2O)_3$ isomers presented in Figure 5 have spectral patterns similar to the experimental spectra except the flat structure labeled 3II (Figure S10 in the SI), which has a large shift and distortion in its spectrum relative to the experimental spectra. The VDE of the flat structure labeled 3II (Figure S10 in the SI) is 6.01 eV, which is higher than the experimental value of 5.7(2) eV. According to the literature, this structure is considered the global minimum.[120]

The cube-like structure (4I in Figure S11 in the SI) is the most stable for n = 4. This structure contains eight hydrogen bonds, the largest number of hydrogen bonds that $NO_3^-(H_2O)_4$ can form. Other structures with seven or eight hydrogen bonds were also found with higher energies than the lowest-energy structure labeled 4I. This structure agrees with the previous theoretical studies.[95,96,122] The most stable geometry of $NO_3^-(H_2O)_5$ possesses a cubic shape (5I in Figure S12 in the SI), which is similar to that of the $(H_2O)_8$ cluster labeled 8I (Figure S7 in the SI). Ten hydrogen bonds form in this structure. The higher-energy structure labeled 5 V (Figure S12 in the SI) was the lowest-energy structure in a previous study.[120] For $NO_3^-(H_2O)_6$ cluster system, the lowest-

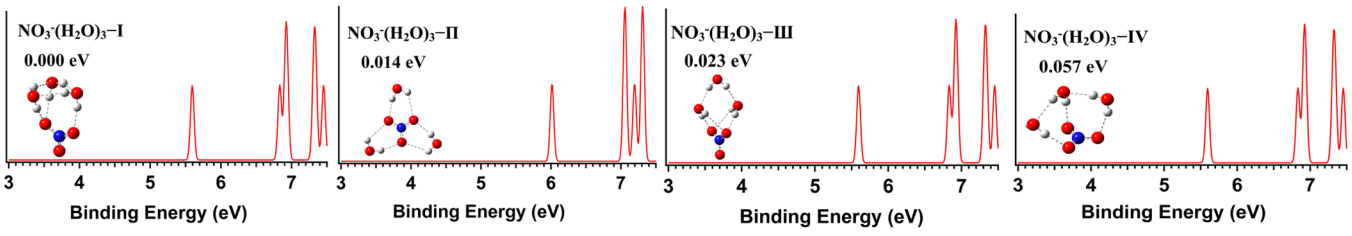

Figure 5. Simulated photoelectron spectra for $NO_3^-(H_2O)_3$. The letters represents the order of the molecular clusters from low energy to high energy for each cluster size.

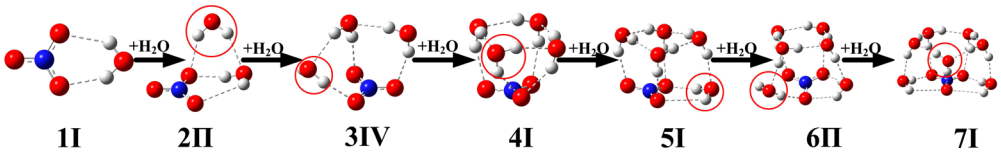

Figure 6. Structural evolution of the $NO_3^-(H_2O)_n$ clusters from n = 1 to 7). One structure's evolutionary path is presented. The inset red ring indicates an added water molecule.

energy structure (6I in Figure S13 in the SI) has one water molecule hydrogen bonded to the cubic-like edge as in the lowest-energy structure of $NO_3^-(H_2O)_5$. This structure contains 11 hydrogen bonds. Other structures with 10 or 11 hydrogen bonds were also found. However, these structures have higher energies than the lowest-energy structure (6I in Figure S13 in the SI). This structure agrees with the previous theoretical studies.[95,96,122] The most stable geometry of $NO_3^-(H_2O)_7$ is a double-five-membered ring structure (7I in Figure S14 in the SI) with 14 hydrogen bonds, which is the maximum number of hydrogen bonds that $NO_3^-(H_2O)_7$ can form. This structure is similar to that of the $(H_2O)_{10}$ cluster labeled 10I (Figure S9 in the SI). This structure agrees with the previous theoretical studies.[95,96,122]

To obtain detailed information regarding cluster growth, we observed the evolution of the $NO_3^-(H_2O)_n$ clusters from n = 1 to 7 in Figure 6, which primarily includes the lowest-energy structures. Beginning with n = 1, two hydrogens from a water molecule bonded to the oxygen of the nitrate anion to form 1I (Figure S10 in the SI); then, another water molecule vertically bonded to the oxygen of the nitrate anion 1I to form 2II (Figure S10 in the SI). Next, a third hydrogen from a water molecule bonded to the oxygen of the nitrate anion to form 3IV (Figure S10 in the SI). For 4I (Figure S11 in the SI), four water molecules formed a square structure above the nitrate anion; then, four hydrogen atoms bonded to three oxygen atoms from the nitrate anion to form four hydrogen bonds. This structure can be easily generated from 3IV (Figure S10 in the SI) by adding one water molecule. One water molecule hydrogen bonded to the nitrate anion to form the two hydrogen bonds found on 4I (Figure S11 in the SI) to obtain structures 4I (Figure S11 in the SI) to 5I (Figure S12 in the SI). The evolution of the 5I structure (Figure S12 in the SI) into 6II (Figure S13 in the SI) can be obtained by adding one water molecule to form one hydrogen bond with the nitrate anion. A hydrogen bond within 6II was broken and two water molecules at the edges of 6II formed two additional hydrogen bonds to obtain the 7I (Figure S14 in the SI) structure.

C. Oxalate + Water Clusters. The lowest-energy structures of $C_2O_4^{2-}(H_2O)_n$ (n = 1–6) are presented in Figure 7. Table 2 provides the calculated VDEs of all of the lowest-energy structures for each cluster size compared with the experimental results.[98] The theoretical results indicated that the $C_2O_4^{2-}(H_2O)_n$ cluster molecules with n = 1 to 2 are electronically unstable: the calculated VDEs are −0.52 and −0.12. The solvated cluster, $C_2O_4^{2-}(H_2O)_3$, has a VDE of 0.51 eV. A minimum of three H_2O molecules is required to stabilize the $C_2O_4^{2-}$ core, and this result is similar to that of the previous study.[98] Two new lowest-energy structures were reported herein for n = 5 and 6, and their coordinates can be obtained in SI. For the lowest-energy structure with n = 1–4, each of the water molecules is bonded to the $C_2O_4^{2-}$ core via two hydrogen bonds. These results are in agreement with the literature.[98,100] At n = 5, water–water hydrogen bonding

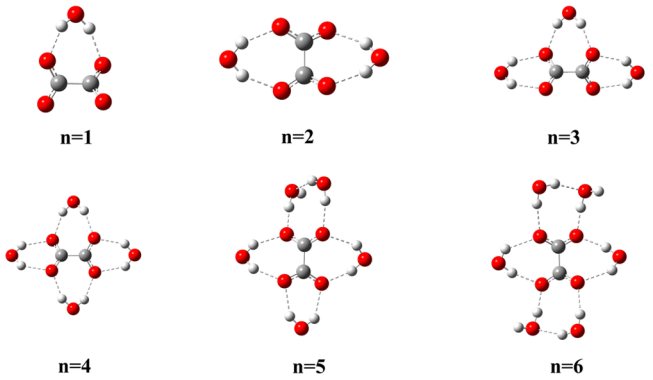

Figure 7. Lowest energy structures of the $C_2O_4^{2-}(H_2O)_n$ (n = 1–6) clusters. The dashed lines represent hydrogen bonds.

Table 2. Experimental and Calculated Values [in electron volts (eV)] of the First Vertical Detachment Energies (VDEs) of the $C_2O_4^{2-}(H_2O)_n$ clusters (n = 1–6)[a]

		VDE	
cluster	N_{HB}	theor	expt[b]
$C_2O_4^{2-}(H_2O)_1$	2	−0.52	
$C_2O_4^{2-}(H_2O)_2$	4	−0.12	
$C_2O_4^{2-}(H_2O)_3$	6	0.51	0.50
$C_2O_4^{2-}(H_2O)_4$	8	1.11	1.14
$C_2O_4^{2-}(H_2O)_5$	9	1.51	1.43
$C_2O_4^{2-}(H_2O)_6$	10	1.83	1.84

[a]All theoretical values were calculated at the B3LYP/aug-cc-pVTZ level. The N_{HB} values represent the number of hydrogen bonds for the $C_2O_4^{2-}(H_2O)_n$ clusters (n = 1–6). The isomer information for each cluster size can be found in the SI. [b]Ref 98.

occurs. The fifth water forms one hydrogen bond with an oxalate and another hydrogen bond with a neighboring water, which forms only one hydrogen bond with the $C_2O_4^{2-}$. To form 5I (Figure S17 in the SI), a hydrogen bond within the 4I is broken, which then forms another water–water hydrogen bond with the fifth water molecule. The lowest-energy structure (5I in Figure S17 in the SI) contains nine hydrogen bonds and is inconsistent with that predicted from the literature.[98,100] For n = 6, the sixth H_2O interacts with the $C_2O_4^{2-}$ via one hydrogen bond and forms another hydrogen bond with a neighboring water. This formation is similar to that of 5I, in which a hydrogen bond within the 5I is broken to allow water–water hydrogen bonding. This structure contains 10 hydrogen bonds, which is inconsistent with that predicted from the literature.[98,100] Other low-energy isomers are also found for the $C_2O_4^{2-}(H_2O)_n$ (n = 1–6) clusters with higher energies than the lowest-energy structure (Figures S15–S18 in the SI) for each cluster size. A possible evolutionary route is presented in Figure 8, which depicts the growth process of $C_2O_4^{2-}(H_2O)_n$ (n = 1–6) clusters achieved through a step-by-step addition of water molecules. Beginning with n = 1–4, each water molecule

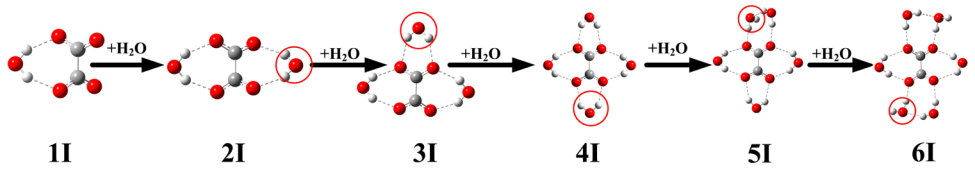

Figure 8. Structural evolution of the $C_2O_4^{2-}(H_2O)_n$ clusters from n = 1 to 6. One structure's evolutionary path is presented. The inset red ring indicates an added water molecule.

hydrogen bonded to the oxalate ion forming two hydrogen bonds. At n = 5 and 6, water−water hydrogen bond appears through a similar formation process by breaking one hydrogen bond between the water and the $C_2O_4^{2-}$ core to form a water−water hydrogen bond.

IV. CONCLUSIONS

In conclusion, a detailed investigation of the structures and isomers of water, nitrate + water, and oxalate + water clusters using basin hopping combined with density functional theory was reported. The compressed sampling technique was used in conjunction with the BH method. We explain the effectiveness of our program using eight separate runs to determine the global minimum for each size cluster. For example, the structures of interest for the $(H_2O)_6$ cluster — the trigonal prism (6I in Figure S5 in the SI), book-like structure (6II in Figure S5 in the SI), cage (6 V in Figure S5 in the SI), cyclic ring (6VI in Figure S5 in the SI), and so on — can be explored in each search. The structures of the water clusters determined using our program are in good agreement with those reported in the literature. According to our calculations, the lowest-energy structure of the $NO_3^-(H_2O)_3$ cluster has a 3D configuration (3I in Figure S10 in the SI), not the flat structure previously reported as the lowest-energy structure by other researchers. The lowest-energy structures of the $NO_3^-(H_2O)_5$ and $NO_3^-(H_2O)_7$ clusters were found to have structures similar to those of pure $(H_2O)_8$ and $(H_2O)_{10}$ clusters. The lowest-lying isomers of the $C_2O_4^{2-}(H_2O)_n$ solvated clusters for n values up to 4 are consistent with those previously reported. Using our program, we also found two different lowest-energy structures (5I in Figure S17 in the SI, 6I in Figure S18 in the SI) for $C_2O_4^{2-}(H_2O)_5$ and $C_2O_4^{2-}(H_2O)_6$.

Combining the basin-hopping method with compressed sampling provides an effective strategy for exploring the minima from one basin to another on complex PESs. This method can be applied to atomic or molecular cluster systems.

■ ASSOCIATED CONTENT

Supporting Information

Predicted low-energy structures of the H_2O_n (n = 4−10), $NO_3^-(H_2O)_n$ (n = 1−7), and $C_2O_4^{2-}(H_2O)_n$ (n = 1−6) clusters using the basin-hopping method combined with density functional theory. This material is available free of charge via the Internet at http://pubs.acs.org.

■ AUTHOR INFORMATION

Corresponding Author

*E-mail: huangwei6@ustc.edu.cn, wjzhang@aiofm.ac.cn.

Notes

The authors declare no competing financial interest.

■ ACKNOWLEDGMENTS

Theoretical work was supported by the National Natural Science Foundation of China (Grant No. 21073196), the State Key Program of National Natural Science of China (Grant No. 21133008), the Director Foundation of AIOFM (Y23H161131), and the Chinese Academy of Sciences. Acknowledgement is also made to the Thousand Youth Talents Plan. Some of the computations were performed at the Supercomputing Center of the Chinese Academy of Sciences and the Supercomputing Center of USTC.

■ REFERENCES

(1) Taylor, K. J.; Pettiettehall, C. L.; Cheshnovsky, O.; Smalley, R. E. *J. Chem. Phys.* **1992**, *96*, 3319−3329.
(2) Furche, F.; Ahlrichs, R.; Weis, P.; Jacob, C.; Gilb, S.; Bierweiler, T.; Kappes, M. M. *J. Chem. Phys.* **2002**, *117*, 6982−6990.
(3) Weis, P. *Int. J. Mass Spectrom.* **2005**, *245*, 1−13.
(4) Fielicke, A.; Kirilyuk, A.; Ratsch, C.; Behler, J.; Scheffler, M.; von Helden, G.; Meijer, G. *Phys. Rev. Lett.* **2004**, *93*, 023401.
(5) Gruene, P.; Rayner, D. M.; Redlich, B.; van der Meer, A. F. G.; Lyon, J. T.; Meijer, G.; Fielicke, A. *Science* **2008**, *321*, 674−676.
(6) Xing, X.; Yoon, B.; Landman, U.; Parks, J. H. *Phys. Rev. B* **2006**, *74*, 165423−165428.
(7) Wales, D. J.; Doye, J. P. *J. Chem. Phys.* **2003**, *119*, 12409.
(8) Stillinger, F. H.; Weber, T. A. *Science* **1984**, *225*, 983−989.
(9) Deaven, D. M.; Ho, K. M. *Phys. Rev. Lett.* **1995**, *75*, 288−291.
(10) Gregurick, S. K.; Alexander, M. H.; Hartke, B. *J. Chem. Phys.* **1996**, *104*, 2684.
(11) Niesse, J. A.; Mayne, H. R. *J. Chem. Phys.* **1996**, *105*, 4700.
(12) Niesse, J. A.; Mayne, H. R. *J. Comput. Chem.* **1997**, *18*, 1233−1244.
(13) Rata, I.; Shvartsburg, A. A.; Horoi, M.; Frauenheim, T.; Siu, K. W. M.; Jackson, K. A. *Phys. Rev. Lett.* **2000**, *85*, 546−549.
(14) Lloyd, L. D.; Johnston, R. L.; Salhi, S. *J. Comput. Chem.* **2005**, *26*, 1069−78.
(15) Alexandrova, A. N. *J. Phys. Chem. A* **2010**, *114*, 12591−12599.
(16) Logsdail, A. J.; Li, Z. Y.; Johnston, R. L. *J. Comput. Chem.* **2012**, *33*, 391−400.
(17) Kirkpatrick, S.; Vecchi, M. *Science* **1983**, *220*, 671−680.
(18) David, J.; Doye, J. P. K. *J. Phys. Chem. A* **1997**, *101*, 5111−5116.
(19) Huang, W.; Pal, R.; Wang, L. M.; Zeng, X. C.; Wang, L. S. *J. Chem. Phys.* **2010**, *132*, 054305.
(20) Li, Z. Q.; Scheraga, H. A. *Proc. Natl. Acad. Sci. U. S. A.* **1987**, *84*, 6611−6615.
(21) Iwamatsu, M.; Okabe, Y. *Chem. Phys. Lett.* **2004**, *399*, 396−400.
(22) Oakley, M. T.; Johnston, R. L.; Wales, D. J. *Phys. Chem. Chem. Phys.* **2013**, *15*, 3965.
(23) Goedecker, S. *J. Chem. Phys.* **2004**, *120*, 9911.
(24) Kim, H. G.; Choi, S. K.; Lee, H. M. *J. Chem. Phys.* **2008**, *128*, 144702.
(25) Shanker, S.; Bandyopadhyay, P. *J. Phys. Chem. A* **2011**, *115*, 11866−75.
(26) Rossi, G.; Ferrando, R. *J. Phys.: Condens. Matter.* **2009**, *21*, 084208.
(27) Zhan, L.; Chen, J.; Liu, W.-K. *Phys. Rev. E* **2006**, *73*, 015701−015704.

(28) Hansmann, U.; Wille, L. *Phys. Rev. Lett.* **2002**, *88*, 068105−068108.
(29) Zhang, R.; Khalizov, A.; Wang, L.; Hu, M.; Xu, W. *Chem. Rev.* **2012**, *112*, 1957−2011.
(30) Kavouras, I. G.; Mihalopoulos, N.; Stephanou, E. G. *Nature* **1998**, *395*, 683−686.
(31) Kulmala, M.; Pirjola, U.; Makela, J. M. *Nature* **2000**, *404*, 66−69.
(32) O'Dowd, C. D.; Aalto, P.; Hameri, K.; Kulmala, M.; Hoffmann, T. *Nature* **2002**, *416*, 497−498.
(33) Kulmala, M. *Science* **2003**, *302*, 1000−1001.
(34) Sipila, M.; Berndt, T.; Petaja, T.; Brus, D.; Vanhanen, J.; Stratmann, F.; Patokoski, J.; Mauldin, R. L., III; Hyvarinen, A.-P.; Lihavainen, H.; Kulmala, M. *Science* **2010**, *327*, 1243−1246.
(35) Zhang, R. *Science* **2010**, *328*, 1366−1367.
(36) Zhang, R. Y.; Suh, I.; Zhao, J.; Zhang, D.; Fortner, E. C.; Tie, X. X.; Molina, L. T.; Molina, M. J. *Science* **2004**, *304*, 1487−1490.
(37) Niedner-Schatteburg, G.; Bondybey, V. E. *Chem. Rev.* **2000**, *100*, 4059−4086.
(38) Delley, B. *J. Chem. Phys.* **1990**, *92*, 508−517.
(39) Frisch, M. J.; Trucks, G. W.; Schlegel, H. B.; Scuseria, G. E.; Robb, M. A.; Cheeseman, J. R.; Scalmani, G.; Barone, V.; Mennucci, B.; Petersson, G. A.; Nakatsuji, H.; Caricato, M.; Li, X.; Hratchian, H. P.; Izmaylov, A. F.; Bloino, J.; Zheng, G.; Sonnenberg, J. L.; Hada, M.; Ehara, M.; Toyota, K.; Fukuda, R.; Hasegawa, J.; Ishida, M.; Nakajima, T.; Honda, Y.; Kitao, O.; Nakai, H.; Vreven, T.; Montgomery, J. A., Jr.; Peralta, J. E.; Ogliaro, F.; Bearpark, M.; Heyd, J. J.; Brothers, E.; Kudin, K. N.; Staroverov, V. N.; Kobayashi, R.; Normand, J.; Raghavachari, K.; Rendell, A.; Burant, J. C.; Iyengar, S. S.; Tomasi, J.; Cossi, M.; Rega, N.; Millam, N. J.; Klene, M.; Knox, J. E.; Cross, J. B.; Bakken, V.; Adamo, C.; Jaramillo, J.; Gomperts, R.; Stratmann, R. E.; Yazyev, O.; Austin, A. J.; Cammi, R.; Pomelli, C.; Ochterski, J. W.; Martin, R. L.; Morokuma, K.; Zakrzewski, V. G.; Voth, G. A.; Salvador, P.; Dannenberg, J. J.; Dapprich, S.; Daniels, A. D.; Farkas, Ö.; Foresman, J. B.; Ortiz, J. V.; Cioslowski, J.; Fox, D. J. *Gaussian 09*, revision A.02; Gaussian, Inc.: Wallingford CT, 2009.
(40) Kendall, R. A.; Apra, E.; Bernholdt, D. E.; Bylaska, E. J.; Dupuis, M.; Fann, G. I.; Harrison, R. J.; Ju, J. L.; Nichols, J. A.; Nieplocha, J.; Straatsma, T. P.; Windus, T. L.; Wong, A. T. *Comput. Phys. Commun.* **2000**, *128*, 260−283.
(41) Woods, E.; Heylman, K. D.; Gibson, A. K.; Ashwell, A. P.; Rossi, S. R. *J. Phys. Chem. A* **2013**, *117*, 4214−4222.
(42) Zhang, T.; Cao, J.; Tie, X.; Shen, Z.; Liu, S.; Ding, H.; Han, Y.; Wang, G.; Ho, K.; Qiang, J. *Atoms. Res.* **2011**, *102*, 110−119.
(43) Laluraj, C.; Thamban, M.; Naik, S.; Redkar, B.; Chaturvedi, A.; Ravindra, R. *The Holocene* **2011**, *21*, 351−356.
(44) Gao, X.; Yang, L.; Cheng, S.; Gao, R.; Zhou, Y.; Xue, L.; Shou, Y.; Wang, J.; Wang, X.; Nie, W. *Atoms. Environ.* **2011**, *45*, 6048−6056.
(45) Cheng, S.; Yang, L.; Zhou, X.; Wang, Z.; Zhou, Y.; Gao, X.; Nie, W.; Wang, X.; Xu, P.; Wang, W. *J. Environ. Monit.* **2011**, *13*, 1662−1671.
(46) Xu, Y.; Nadykto, A. B.; Yu, F.; Jiang, L.; Wang, W. *J. Mol. Struct: THEOCHEM* **2010**, *951*, 28−33.
(47) Drenck, K.; Hvelplund, P.; Nielsen, S. B.; Panja, S.; Støchkel, K. *Int. J. Mass. Spectrom.* **2008**, *273*, 126−131.
(48) Ramazan, K.; Wingen, L. M.; Miller, Y.; Chaban, G. M.; Gerber, R. B.; Xantheas, S. S.; Finlayson-Pitts, B. J. *J. Phys. Chem. A* **2006**, *110*, 6886−6897.
(49) Noda, J.; Ljungström, E. *Atmos. Environ.* **2002**, *36*, 521−525.
(50) Li, X.; Qin, D.; Zhou, H. *Chin. Sci. Bull.* **2001**, *46*, 80−83.
(51) Thompson, L. G. *Quat. Sci. Rev.* **2000**, *19*, 19−35.
(52) Atkinson, R. *Atmos. Environ.* **2000**, *34*, 2063−2101.
(53) Hallquist, M.; WÄngberg, I.; LjungstrÖm, E. *Environ. Sci. Technol.* **1997**, *31*, 3166−3172.
(54) Ludwig, R. *Angew. Chem., Int. Ed.* **2001**, *40*, 1808−1827.
(55) Shields, R. M.; Temelso, B.; Archer, K. A.; Morrell, T. E.; Shields, G. C. *J. Phys. Chem. A* **2010**, *114*, 11725−11737.
(56) Takeuchi, H. *J. Chem. Inf. Model.* **2008**, *48*, 2226−2233.
(57) Goken, E. G.; Joshi, K. L.; Russo, M. F., Jr.; van Duin, A. C.; Castleman, A. W., Jr. *J. Phys. Chem. A* **2011**, *115*, 4657−64.
(58) Bandyopadhyay, P. *Chem. Phys. Lett.* **2010**, *487*, 133−138.
(59) James, T.; Wales, D. J.; Hernández-Rojas, J. *Chem. Phys. Lett.* **2005**, *415*, 302−307.
(60) Wales, D. J.; Hodges, M. P. *Chem. Phys. Lett.* **1998**, *286*, 65−72.
(61) Kabrede, H.; Hentschke, R. *J. Phys. Chem. B* **2003**, *107*, 3914−3920.
(62) Yoo, S.; Aprà, E.; Zeng, X. C.; Xantheas, S. S. *J. Phys. Chem. Lett.* **2010**, *1*, 3122−3127.
(63) Li, F.; Liu, Y.; Wang, L.; Zhao, J.; Chen, Z. *Theor. Chem. Acc.* **2012**, *131*, 1163.
(64) Coe, J. V.; Lee, G. H.; Eaton, J. G.; Arnold, S. T.; Sarkas, H. W.; Bowen, K. H.; Ludewigt, C.; Haberland, H.; Worsnop, D. R. *J. Chem. Phys.* **1990**, *92*, 3980.
(65) Kazimirski, J. K.; Buch, V. *J. Phys. Chem. A* **2003**, *107*, 9762−9775.
(66) Buck, U.; Ettischer, I.; Melzer, M.; Buch, V.; Sadlej, J. *Phys. Rev. Lett.* **1998**, *80*, 2578−2581.
(67) Maheshwary, S.; Patel, N.; Sathyamurthy, N.; Kulkarni, A. D.; Gadre, S. R. *J. Phys. Chem. A* **2001**, *105*, 10525−10537.
(68) Khan, A. *J. Phys. Chem. A* **1999**, *103*, 1260−1264.
(69) Khan, A. *J. Chem. Phys.* **1997**, *106*, 5537.
(70) Young, R. M.; Yandell, M. A.; King, S. B.; Neumark, D. M. *J. Chem. Phys.* **2012**, *136*, 094304.
(71) Rai, D.; Kulkarni, A. D.; Gejji, S. P.; Pathak, R. K. *J. Chem. Phys.* **2008**, *128*, 034310.
(72) Wang, Y.; Babin, V.; Bowman, J. M.; Paesani, F. *J. Am. Chem. Soc.* **2012**, *134*, 11116−9.
(73) Temelso, B.; Koeddermann, T.; Kirschner, K. N.; Klein, K.; Shields, G. C. *Comput. Theor. Chem.* **2013**, *1021*, 240−248.
(74) Pérez, C.; Lobsiger, S.; Seifert, N. A.; Zaleski, D. P.; Temelso, B.; Shields, G. C.; Kisiel, Z.; Pate, B. H. *Chem. Phys. Lett.* **2013**, *571*, 1−15.
(75) Pérez, C.; Muckle, M. T.; Zaleski, D. P.; Seifert, N. A.; Temelso, B.; Shields, G. C.; Kisiel, Z.; Pate, B. H. *Science* **2012**, *336*, 897−901.
(76) Saykally, R. J.; Wales, D. J. *Science* **2012**, *336*, 814−815.
(77) Temelso, B.; Archer, K. A.; Shields, G. C. *J. Phys. Chem. A* **2011**, *115*, 12034−12046.
(78) Temelso, B.; Shields, G. C. *J. Chem. Theory. Comput.* **2011**, *7*, 2804−2817.
(79) Shields, G. C.; Kirschner, K. N. *Synth. React. Inorg. Met.-Org. Chem.* **2008**, *38*, 32−39.
(80) Dunn, M. E.; Evans, T. M.; Kirschner, K. N.; Shields, G. C. *J. Phys. Chem. A* **2006**, *110*, 303−309.
(81) Dunn, M. E.; Pokon, E. K.; Shields, G. C. *Int. J. Quantum Chem.* **2004**, *100*, 1065−1070.
(82) Dunn, M. E.; Pokon, E. K.; Shields, G. C. *J. Am. Chem. Soc.* **2004**, *126*, 2647−2653.
(83) Day, M. B.; Kirschner, K. N.; Shields, G. C. *J. Phys. Chem. A* **2005**, *109*, 6773−6778.
(84) Day, M. B.; Kirschner, K. N.; Shields, G. C. *Int. J. Quantum Chem.* **2005**, *102*, 565−572.
(85) Belair, S. D.; Francisco, J. S. *Phys. Rev. A.* **2003**, *67*, 063206.
(86) McDonald, S.; Ojamäe, L.; Singer, S. J. *J. Phys. Chem. A* **1998**, *102*, 2824−2832.
(87) Ohtaki, H.; Radnai, T. *Chem. Rev.* **1993**, *93*, 1157−1204.
(88) Nakahara, M.; Emi, K. *J. Chem. Phys.* **1993**, *99*, 5418−5425.
(89) Bergstrom, P. A.; Lindgren, J.; Kristiansson, O. *J. Phys. Chem.* **1991**, *95*, 8575−8580.
(90) Ikushima, Y.; Saito, N.; Arai, M. *J. Phys. Chem. B* **1998**, *102*, 3029−3035.
(91) Waterland, M. R.; Stockwell, D.; Kelley, A. M. *J. Chem. Phys.* **2001**, *114*, 6249−6258.
(92) Shen, M. Z.; Xie, Y. M.; Schaefer, H. F.; Deakyne, C. A. *J. Chem. Phys.* **1990**, *93*, 3379−3388.
(93) Howell, J. M.; Sapse, A. M.; Singman, E.; Synder, G. *J. Phys. Chem.* **1982**, *86*, 2345−2349.
(94) Narcisi, R. S.; Bailey, A. D.; Lucca, L. D.; Sherman, C.; Thomas, D. M. *J. Atmos. Terr. Phys.* **1971**, *33*, 1147.

(95) Goebbert, D. J.; Garand, E.; Wende, T.; Bergmann, R.; Meijer, G.; Asmis, K. R.; Neumark, D. M. *J. Phys. Chem. A* **2009**, *113*, 7584−7592.
(96) Pathak, A.; Mukherjee, T.; Maity, D. *J. Phys. Chem. A* **2008**, *112*, 3399−3408.
(97) Lebrero, M. C. G.; Bikiel, D. E.; Elola, M. D.; Estrin, D. A.; Roitberg, A. E. *J. Chem. Phys.* **2002**, *117*, 2718.
(98) Wang, X.-B.; Yang, X.; Nicholas, J. B.; Wang, L.-S. *J. Chem. Phys.* **2003**, *119*, 3631.
(99) Weber, K. H.; Morales, F. J.; Tao, F.-M. *J. Phys. Chem. A* **2012**, *116*, 11601−11617.
(100) Rosas-García, V. M.; del Carmen Sáenz-Tavera, I.; Rodríguez-Herrera, V. J.; Garza-Campos, B. R. *J. Mol. Model.* **2013**, 1−13.
(101) Gao, B.; Liu, Z.-f. *J. Phys. Chem. A* **2005**, *109*, 9104−9111.
(102) Yokouchi, Y.; Ambe, Y. *Atmos. Environ.* **1986**, *20*, 1727−1734.
(103) Kawamura, K.; Ikushima, K. *Environ. Sci. Technol.* **1993**, *27*, 2227−2235.
(104) Kawamura, K.; Kasukabe, H.; Barrie, L. A. *Atmos. Environ.* **1996**, *30*, 1709−1722.
(105) Xu, W.; Zhang, R. *J. Phys. Chem. A* **2012**, *116*, 4539−4550.
(106) Huang, W.; Sergeeva, A. P.; Zhai, H. J.; Averkiev, B. B.; Wang, L. S.; Boldyrev, A. I. *Nat. Chem.* **2010**, *2*, 202−206.
(107) Huang, W.; Wang, L.-S. *Phys. Rev. Lett.* **2009**, *102*, 153401−153404.
(108) Huang, W.; Zhai, H. J.; Wang, L. S. *J. Am. Chem. Soc.* **2010**, *132*, 4344−4351.
(109) Huang, W.; Ji, M.; Dong, C. D.; Gu, X.; Wang, L. M.; Gong, X. G.; Wang, L. S. *ACS Nano* **2008**, *2*, 897−904.
(110) Do, H.; Besley, N. A. *J. Chem. Phys.* **2012**, *137*, 134106.
(111) Rapacioli, M.; Calvo, F.; Spiegelman, F.; Joblin, C.; Wales, D. J. *J. Phys. Chem. A* **2005**, *109*, 2487−2497.
(112) Li, F.; Wang, L.; Zhao, J.; Xie, J. R.-H.; Riley, K. E.; Chen, Z. *Theor. Chem. Acc.* **2011**, *130*, 341−352.
(113) Shields, R. M.; Temelso, B.; Archer, K. A.; Morrell, T. E.; Shields, G. C. *J. Phys. Chem. A* **2010**, *114*, 11725−11737.
(114) Xu, K.-M.; Huang, T.; Wen, H.; Liu, Y.-R.; Gai, Y.-B.; Zhang, W.-J.; Huang, W. *RSC Adv.* **2013**, *3*, 24492−24502.
(115) Huang, W.; Bulusu, S.; Pal, R.; Zeng, X. C.; Wang, L.-S. *ACS Nano* **2009**, *3*, 1225−1230.
(116) Huang, W.; Bulusu, S.; Pal, R.; Zeng, X. C.; Wang, L.-S. *J. Chem. Phys.* **2009**, *131*, 234305−234311.
(117) Wawak, R. J.; Wimmer, M. M.; Scheraga, H. A. *J. Phys. Chem.* **1992**, *96*, 5138−5145.
(118) Liu, K.; Brown, M. G.; Carter, C.; Saykally, R. J.; Gregory, J. K.; Clary, D. C. *Nature* **1996**, *381*, 501−503.
(119) Nauta, K.; Miller, R. E. *Science* **2000**, *287*, 293−295.
(120) Wang, X.-B.; Yang, X.; Wang, L.-S.; Nicholas, J. B. *J. Chem. Phys.* **2002**, *116*, 561.
(121) Waterland, M. R.; Stockwell, D.; Kelley, A. M. *J. Chem. Phys.* **2001**, *114*, 6249.
(122) Pathak, A. K. *Chem. Phys.* **2011**, *384*, 52−56.